

elements Mo, W, Cu and N, for example [1–3]. These grades of materials has a microstructure composed by two phases, austenite (γ – Face Centred Cubic, FCC) and ferrite (α – Body Centred Cubic, BCC), in about 1:1 proportion.

Regarding the corrosion resistance of these steels, researches have pointed critical aspects concerning the susceptibility to localized corrosion and stress corrosion cracking in environments containing different partial pressures of CO_2 and H_2S ($\text{P}_{\text{CO}_2}/\text{PH}_2\text{S}$). The increasing of both corrosion processes is commonly related to microstructure changes as consequence of heat treatments or welding procedures. Kiochy et al., 2012 [4], presented results showing the deleterious impact of intermetallic phases on localized corrosion resistance of a superduplex stainless steel UNS S32760. In that work, the authors applied the double loop electrochemical potentiodynamic reactivation (DL-EPR) technique, according ISO 12732 standard [5], to correlate the increase in the susceptibility of localized corrosion with the presence of deleterious phases.

The qualification of welding procedure for this kind of steel requires evaluation of the resistance to cracking through tests according to ISO 7539-2 [6] and NACE MR 0175/ISO 15156-3 [7]. These standard together covers stress corrosion tests in sour solution containing H_2S . Chehuan et al., 2014 [8], have used the procedure described in ISO 7539-2 standard to evaluate the influence of secondary austenite (γ_2) on the stress sulphide cracking (SSC) of welded joints of super duplex stainless steel (UNS S32750). It was verified that the simple presence of γ_2 does not necessarily imply in loss of corrosion resistance, its effect seems to be related to the precipitation region in the matrix and temperature range in which this phase forms.

However, tests according ISO 7539-2 and NACE MR 0175/ISO 15156-3 do not provide information that can be used in engineering of critical analysis to determine the remaining life of a metallic component or structure. The results are used only for qualitative rating due to a greater or lesser stress corrosion cracking susceptibility. Thus, the development of methodologies enabling to apply the elastic–plastic or elastic-linear fracture mechanics theories in presence of quasi-static or dynamic loading and corrosive environment become indispensable for a quantitative analysis of the risk to failure. Indeed, the evaluation of the BS 7448 parts 1 [9] and 2 [10], BS ISO EN 15653 [11], ASTM E1290-07 [12] or ASTM E1820-08 [13] standards for application in corrosive environment to obtain a quantitative parameter (Critical Tip Open Displacement, CTOD, or J Integral) become a technical alternative for reliable analysis of loss of toughness on metallic materials.

Olden et al. [14] presented results about the diffusion coefficient of hydrogen in different microstructures. They found values of $10^{-5} \text{ m}^2 \text{ s}^{-1}$, $10^{-16} \text{ m}^2 \text{ s}^{-1}$ and $10^{-15} \text{ m}^2 \text{ s}^{-1}$ respectively for ferrite, austenitic steels and super duplex stainless steel, in charging conditions of 1 mA/cm^2 in solution 0.1 M NaOH . These differences in diffusion coefficient of hydrogen show that in SDSS there is a great solubility to hydrogen (H^0) in austenite phase and a low solubility in ferrite phase. Consequently, the accumulation of hydrogen depends of the ratio between austenite and ferrite phase for this kind of steel and this point is important to be considered to take into account the hydrogen effect in dual phase steels.

Turnbull et al. [15] studied the resistance to hydrogen-assisted cracking of welded supermartensitic stainless steel using a very slow strain rate test (nominally 10^{-8} s^{-1}) under cathodic protection conditions. The authors compared the effect of strain rate and temperature. They concluded that in presence of hydrogen, the strain rate is the main parameter influencing the cracking. Based on Turnbull's results, in our paper we will use a very low strain rate to test the different welded joints.

Sieurim et al. [16] showed fracture toughness results of base and weld metals at subzero temperatures. They used J-integral calculations to full size three point bending samples. The authors correlated the fracture toughness with Charpy impact values and found a transition curve showing the influence of temperature in the fracture toughness.

On fracture mechanics in acid aggressive environment, particularly concerning the hydrogen effect, there is not systematic information about the limits values of fracture toughness that could be used to predict the remaining life or critical defect size in duplex or super duplex stainless steel. Indeed, in acid media the more aggressive agent for these steels is the hydrogen [17,18]. Bahrami et al. [19] presented results related to influence of hydrogen content and strain rates on fracture toughness of pipe and forged parents materials. In general, the reduction of fracture toughness were due presence of hydrogen after cathodic charging and the deleterious effect was more pronounced to displacement rate of 0.006 mm h^{-1} . According the authors, from this value of displacement rate the toughness values do not changes significantly with displacement or strain rate.

John Jy-An Wang et al. [20] showed results concerning development a new methodology to assess the influence of hydrogen through fracture toughness tests with a torsional fixture to spiral notch torsion test (SNTT). The *in situ* tests indicated that the exposure to H_2 significantly reduces the fracture toughness of a high strength steels. Yanfei Wang et al. [21] presented a simple quantitative model to predict the fracture toughness of steels in gaseous hydrogen. The model is based on the assumption that fracture of a crack body occur when the maximum principal stress ahead of crack tip reaches the critical cohesive stress for crack initiation. The model describes also the dependence of fracture toughness on hydrogen pressure, temperature and yield strength of steels. In both cases, the authors do not applied the methodologies specifically on superduplex stainless steels.

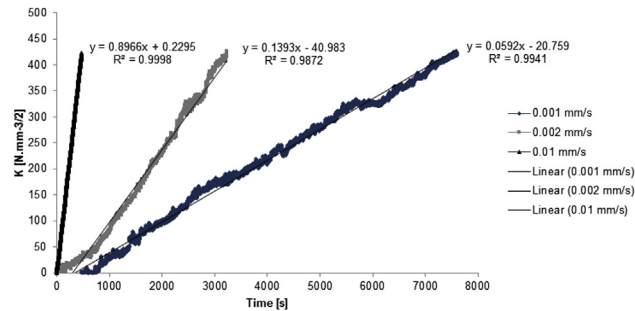
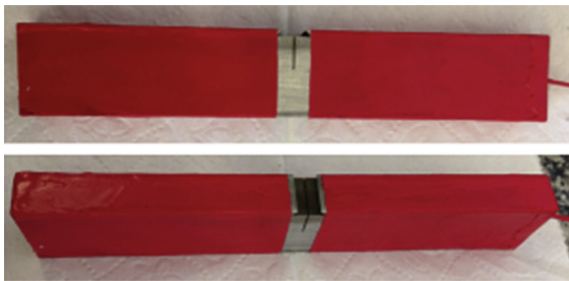
The present work presents results of fracture toughness for two welded joints using different heat inputs, in the presence of hydrogen coming from cathodic protection with different time of hydrogenation. The main purpose is to discuss a coherent methodology to be used to assess the loss of fracture toughness in welded joints of super duplex stainless steel (UNS S32750).

Materials and methods

The SDSS used in this work was a UNS S32750 obtained from a pipe with outside diameter of 203.20 mm and thickness of 19.05 mm. The chemical composition (main elements) and

Table 5 – Dimension of samples machined from welded joint with low heat input.

Heat input	2.0 kJ/mm					
	Air			Hydrogenation		
Condition	2.0 - CP1	2.0 - CP2	2.0 - CP3	2.0 - H1	2.0 - H2	2.0 - H3
Sample						
B (mm)	14.05	15.23	15.29	13.78	13.86	13.94
W (mm)	28.05	29.9	30.13	27.89	27.92	27.95
e (mm)	13.39	13.52	13.51	11.96	12.08	12.05

**Fig. 3 – Tests for three different displacement control of the machine.****Fig. 4 – Samples after coating.**

limitation of flow in servo valve of the machine. The value of loading rate selected for these tests was $0.897 \text{ N mm}^{-3/2} \text{ s}^{-1}$ (0.01 mm min^{-1}). The samples to be charged by hydrogen were coated with a non-conductive layer, as can be seen in Fig. 4, getting exposed only the area of notch. The solution used was 3.5% NaCl and the potential applied was $-1400 \text{ mV}_{\text{SCE}}$ (around -1000 mV of overpotential from the open circuit potential), simulating an excessive cathodic protection, which may occur in subsea application. The initial pH, before application of the cathodic protection, remained between 5.9 and 6.2 and after 96 h to $-1400 \text{ mV}_{\text{SCE}}$ between 5.4 and 5.8.

Table 6 – Principal welding parameter used in the samples welded with low heat input.

Layer	I_m (A)	V_m (V)	V_s (mm/s)	H (kJ/mm)
Root	90	9.5	0.78	1.1
Hot pass	110	9.5	0.95	
Filling	150	9.3	1.27	
Finishing	150	9.3	1.27	

Results and discussion

The main parameters for each welded joint were monitored during the welding and used to calculate the heat inputs. The average values are shown in Tables 6 and 7. The results of the metallographic analysis, quantification of phases and austenitic spacing are presented in Fig. 5, Table 8 and Fig. 6, respectively.

It is possible to observe after metallographic analysis (Fig. 5 and Table 8) a great anisotropy in terms of distribution and morphologies in both samples. Large amounts of austenite *Widmanstatten* and secondary austenite (γ_2) were observed. These results are related to re-heating promoted by subsequent welding passes. It was not observed the presence of deleterious phases and consequently, it is possible to assert that the predominant mechanism to decomposition of ferrite phase in γ_2 was the reaction $\alpha \rightarrow \text{CrN/Cr}_2\text{N} + \gamma_2$. Another important point observed in this analysis was the dispersion found in austenitic spacing, resulting in a relative accuracy higher than the minimum specified by the standard DNV RP F112 08 [23], which is 10%. Another important point about austenitic spacing is that the values found to relative accuracy decrease with the increase of heat input and consequently, with the reduction of reheating. This fact may indicate that this parameter is not appropriate to be used in cases of high microstructural anisotropy, as in welding joints.

Table 9 and Fig. 7 show the CTOD (δ) tests results. However, before discussion about CTOD results, a brief approach will be presented about significance of the stable growth cracking propagation (Δa) and the methodology used to identify and obtain this parameter. For identification and measurement of Δa , firstly is performed a thermal procedure on fracture surface designated by heat tint. This procedure consists of heating the samples to $500 \text{ }^\circ\text{C}$ by 30 min, followed by air cooling. This procedure allows the cracks (fatigue and Δa) to acquire different colors. After that, the same methodology used to measure the cracking fatigue was used to measure Δa . Fig. 8 shows the images before and after heat tint and the methodology used to determine the length of the cracking fatigue (δ) and Δa .

Table 7 – Principal welding parameter used in the samples welded with high heat input.

Layer	I_m (A)	V_m (V)	V_s (mm/s)	H (kJ/mm)
Root	110	9.5	0.52	2.0
Hot pass	120	9.5	0.57	
Filling	170	9.0	0.77	
Finishing	170	9.0	0.77	

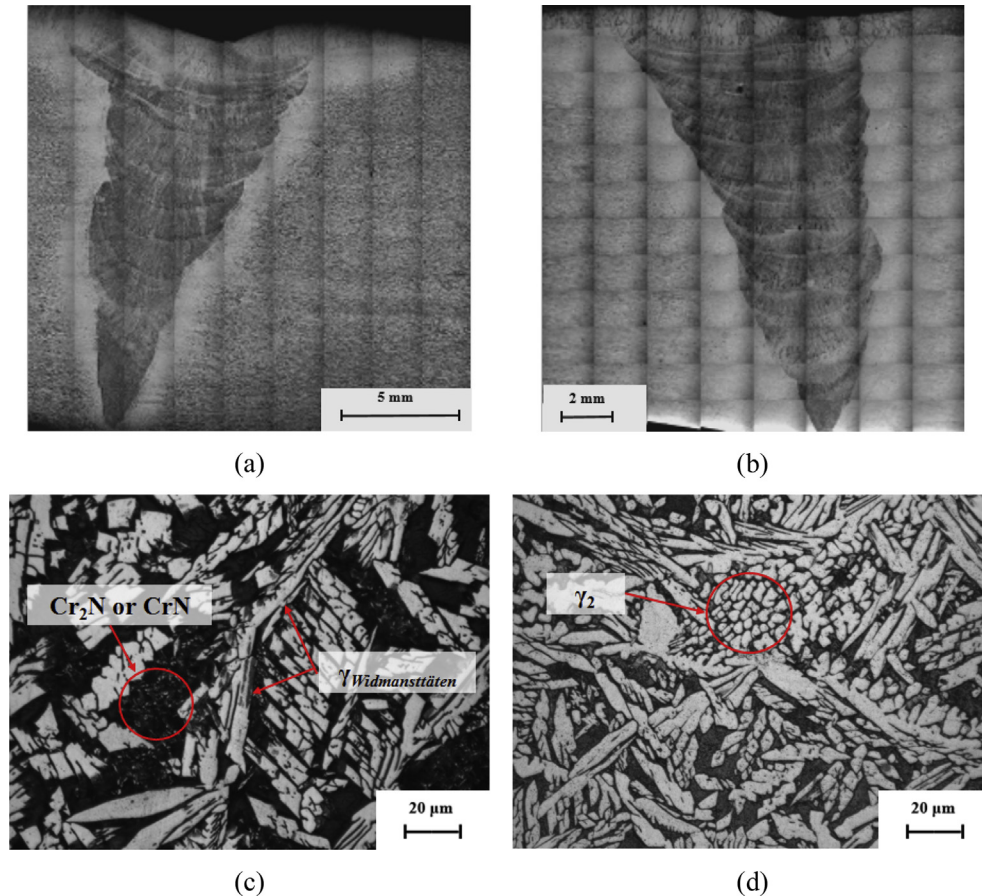


Fig. 5 – Metallographic analysis. Examples of distribution and morphologies of phases found. (a) and (c) sample 1.1 kJ/mm and (b) and (d) 2.0 kJ/mm.

Table 8 – Percentage of phases according ASTM E1245-03 [17] to 95% of confidence interval (95% CI).

1.1 kJ/mm			2.0 kJ/mm		
Sample	% γ	% α	Sample	% γ	% α
Average	42.04	57.96	Average	42.35	57.65
95% CI	1.77	1.77	95% CI	0.32	0.32

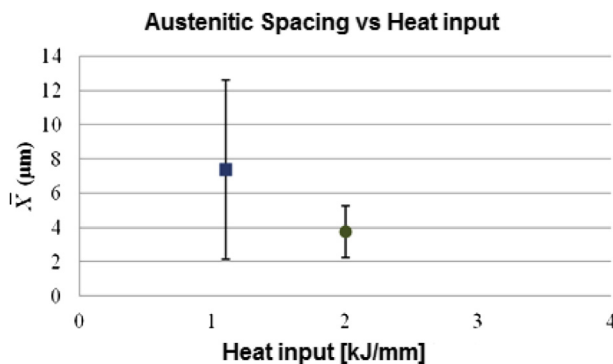


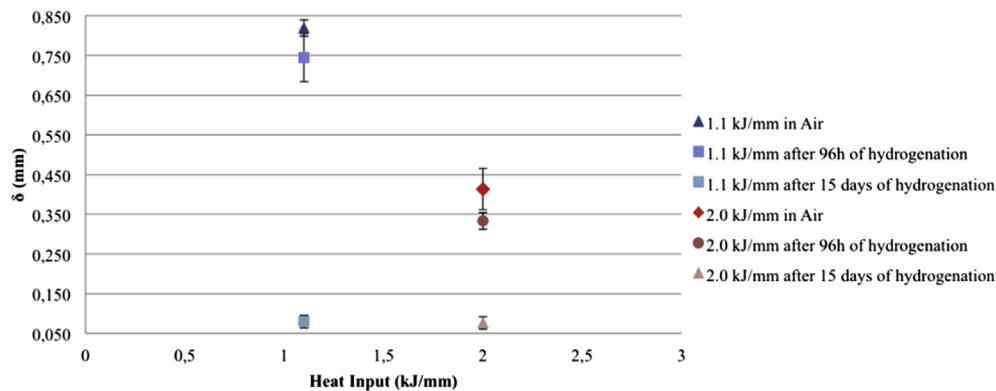
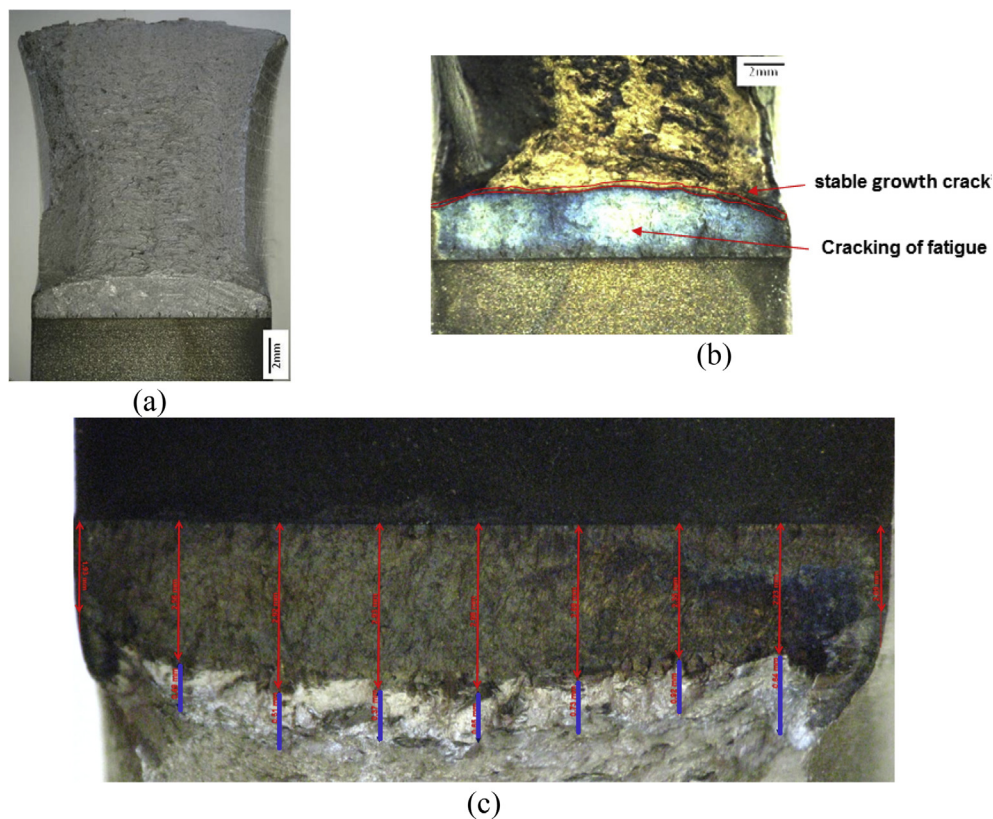
Fig. 6 – Austenitic spacing results according DNV RP F112-08 [19].

In tests performed in air Δa is related to a phenomena called pop-in, which corresponds to the appearance of a brittle crack and will be better discussed during the text. In the presence of pop-in during the test, a graphic instability (abrupt drop in loading) during the CTOD test is observed (Fig. 9). Although predicted in the literature, this phenomenon was not seen in the tests performed in the samples used in the present paper. Indeed, as seen in Fig. 10, the results of δ tests do not present such instability and Δa occurs due to brittle stable growth crack propagation. From these results is possible to note that even without pop-in, there was a significant reduction in CTOD value and stable growth cracking. Moreover, brittle appearance was noted in all samples. The evolution of the predominant fracture micromechanisms found for all samples, as function of hydrogenation time, can be seen in Fig. 11.

The δ values obtained for samples 1.1 kJ mm^{-1} and 2.0 kJ mm^{-1} after hydrogenation must be classified as δ_m , value of CTOD at the first attainment of a maximum force plateau for fully plastic behavior. This fact is crucial because from integrity analysis, the δ values, together with stress analysis, will be used to estimate the critical size defects to be admitted in a practical situation. However, the value of critical size defects obtained in presence of hydrogen can diminish with time of hydrogenation. This fact can be observed in the resistance curve presented in Fig. 12.

Table 9 – Results of the CTOD tests.

Condition		Δa (mm)	δ (mm)
1.1 kJ/mm	Air	–	0.820 ± 0.021
	After 96 h of hydrogenation	0.268 ± 0.014	0.745 ± 0.061
	After 15 days of hydrogenation	0.284 ± 0.003	0.079 ± 0.004
2.0 kJ/mm	Air	–	0.414 ± 0.052
	After 96 h of hydrogenation	0.280 ± 0.005	0.333 ± 0.021
	After 15 days of hydrogenation	0.539 ± 0.012	0.076 ± 0.011

**Fig. 7 – CTOD results by heat input as function of the time hydrogenation.****Fig. 8 – Methodology for measures cracking of fatigue and SGPC. (a) after test, (b) after heat tint and (c) procedure to measure the lengths of the cracks (in red cracks of fatigue and in blue stable growth cracks). (For interpretation of the references to color in this figure legend, the reader is referred to the web version of this article.)**

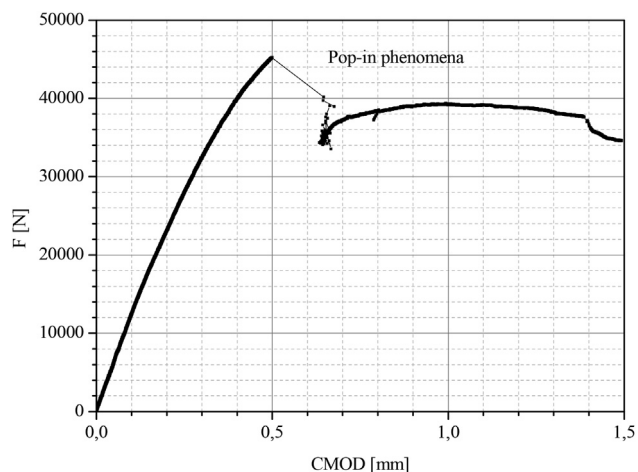


Fig. 9 – Example of graphic instability representative of pop-in.

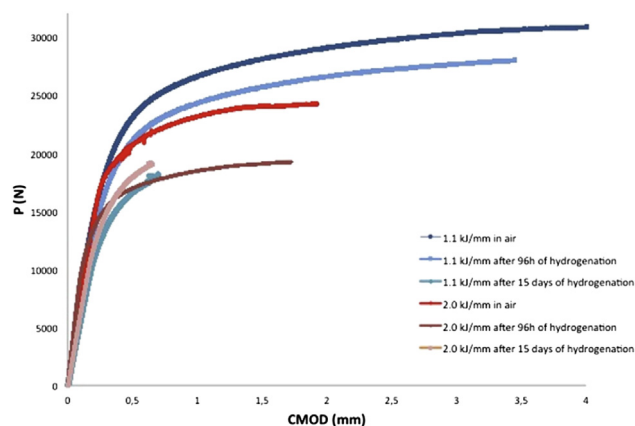


Fig. 10 – Typical graphic aspect obtained during CTOD tests.

As seen, Fig. 12 shows a reduction on δ and J integral when the hydrogenation time increased, for both heat input used: 1.1 kJ mm^{-1} (from $0.820 \text{ mm} \pm 0.021$ – $0.079 \text{ mm} \pm 0.004$) and 2.0 kJ mm^{-1} (from 0.414 ± 0.052 to 0.076 ± 0.011). As consequence, a substantial reduction in plasticity around the critical tip open displacement was observed. It means that the hydrogen eliminates the plastic zone in front of the crack and imposes a limit in the application of the elastic–plastic fracture mechanical theory in the present situation. Indeed, for tests in air, the plasticity of weld metal requires the application of elastic–plastic fracture mechanical theory. Nevertheless, for different hydrogenation times, becomes questionable the use of this theory due the drastic reduction of the plasticity. A comparative procedure using de values of K_{IC} [$\text{MPa m}^{0.5}$] and lower values of δ_m (in this case to δ_m values obtained after 360 h of hydrogenation) could be used to better explicit this situation. The procedure consists in analyze if after 360 h of exposition the δ_m correspond to valid K_{IC} value or not. For this, a value of K_Q [$\text{MPa m}^{0.5}$], is obtained, the factor $2.5 \times (K_Q/\sigma_{YS})^2$ (K_Q and σ_{YS} are the K value related with the

maximum load value and yield stress, respectively) is calculated and if the factor is minor than crack length (a_0), thickness (B) and $W-a_0$ then $K_Q = K_{IC}$. Thus, would be possible to evaluate from a determined length of crack, time of hydrogenation and loading, if would be possible or not to take into account the plasticity around of critical tip open displacement. In addition, this procedure could be used as a criterion to choice which fracture mechanic theory (linear-elastic or elastic–plastic) is safer to be used within the integrity analysis. In Table 10 the values of K_Q and δ_m are presented. Considering the fact that after 96 h of hydrogenation the values of δ_m are 0.745 mm and 0.333 mm to 1.1 kJ mm^{-1} and 2.1 kJ mm^{-1} respectively and the fracture mode were quasi-cleavage for both samples, these results could establish a threshold region of fracture toughness to operate in situation of hydrogen embrittlement: $113.38 \text{ MPa m}^{0.5}$ (Table 10). Below this value the microstructure presents high susceptibility to unstable crack propagation, which could lead to catastrophic failure. These results are coherent with the ones obtained by Brahami at al [19] that arrived practically to the same conclusion for pipe and forged parents materials.

It seems that even after 360 h of exposition, the K_Q values are not the K_{IC} values, but is clearly approaching to this valor. K_Q values about $45 \text{ MPa m}^{0.5}$ the values of a_0 , B and $W-a_0$ are higher than $2.5 \times (K_Q/\sigma_{YS})^2$ and would be characterized a total reduction of plasticity around of critical tip open displacement. Moreover, taking into account that this material has a dual phase structure (α with high diffusivity and γ with high solubility to hydrogen), the plastic deformation around the critical tip open displacement can disappear for longer time of hydrogenation or lower loading rate. Consequently, it seems more reasonable to use tests based on the linear-elastic fracture for this kind of material. This point has already been, implicitly, proposed by Ernst at all [25,26] for sour environments tests, where the authors emphasized the importance in establishing a maximum value of K [$\text{MPa m}^{0.5}$] for which there is no crack growth in a certain time of exposition in environment containing H_2S . Furthermore, the authors presented results showing the necessity to adjust a criterion to describe the effect of hydrogen on fracture toughness. Indeed, when in the crack tip opening stress exceeds a critical concentration of hydrogen the cracks propagate, even with a small plasticity. The authors pointed out that more effort is required to carry out a comprehensive study of the parameters involving in the crack propagation. Indeed, the tests used by the authors concern the linear elastic fracture mechanics concepts. For the authors the unique point to be considered in this case, in the presence of hydrogen, is the minimum load to support the instable growth crack. This aspect is totally in agreement with our paper.

Conclusions

The main conclusions of this work are the following:

- i. The loading rate selected ($0.897 \text{ N mm}^{-3/2} \text{ s}^{-1}$) was slow enough to allowing hydrogen interaction with the process of crystallographic shear at the critical aperture area in the crack tip (δ), reducing the CTOD values for samples welded with 1.1 kJ/mm and with 2.0 kJ/mm ;

Acknowledgements

M.A. Lages thanks FAPERJ for her Msc scholarship.

REFERENCES

- [1] Noble DN. Welding, brazing and soldering. Selection of wrought duplex stainless steels. *ASM Int* 1993;6.
- [2] Alves FP. Estudo da evolução microestrutural de juntas de aço inoxidável superduplex em soldagem TIG orbital com múltiplos passes [Master Thesis]. Rio de Janeiro: Universidade Federal do Rio de Janeiro; 2011.
- [3] Lippold JC, Kotecki DJ. Welding metallurgy and weldability of stainless steels. 1st ed. Wiley-Interscience; 2005.
- [4] Kioshy SA, Flávio VVS, Miranda M, Margarit-Mattos ICP, Vivier V, Mattos OR. Assessment of electrochemical methods used on corrosion of super duplex stainless steel. *Corros Sci* 2012;59:71–80.
- [5] ISO 12732. Corrosion of metals and alloys – electrochemical potentiokinetic reactivation measurement using the double loop method (based on Cihal's method). 2009.
- [6] ISO 7539-2. Aspects of stress corrosion cracking are much discussed in the context of welding for these class of materials. 2009.
- [7] NACE MR 0175/ISO 15156–3. Petroleum and natural gas industries – materials for use in H₂S-containing environments in oil and gas production – Part 3: cracking-resistance CRAs (corrosion-resistant alloys) and others alloys. 2003.
- [8] Chahuan T, Dreilich V, Kioshy SA, Mattos OR. Influence of multipass welding on the corrosion resistance of a superduplex stainless steel subjected to pulsed gas metal arc welding. *Corros Sci* 2014;86:268–74.
- [9] BS 7448-1. Fracture mechanics toughness tests. Method for determination of K_{IC}, critical CTOD and critical J values of metallic materials. 1991.
- [10] BS 7448-2. Fracture mechanics toughness tests. Method for determination of K_{IC}, critical CTOD and critical J values of welds in metallic materials. 1997.
- [11] BS ISO EN 15653. Method of test for the determination of quasistatic fracture toughness of welds. 2010.
- [12] E1290-07. Standard test method for crack-tip opening displacement (CTOD) fracture toughness measurement. 2007.
- [13] ASTM E1820-08. Standard test method for measurement of toughness fracture. 2008.
- [14] Olden V, Thaulow C, Johnsen R. Modelling of hydrogen diffusion and hydrogen induced cracking in supermartensitic and duplex stainless steels. *Mater Des* 2008;29:1934–48.
- [15] Turnbull A, Hinds G. Testing of supermartensitic stainless steel welds under cathodic protection at very low strain rate. *Corrosion* 2005;62:371–4.
- [16] Sieurin H, Sandström R. Fracture toughness of a welded duplex stainless steel. *Eng Fract Mech* 2006;73:377–90.
- [17] Elhoud AM, Renton NC, Deans WF. Hydrogen embrittlement of super duplex stainless steel in acid solution. *Int J Hydrogen Energy* 2010;35:6455–64.
- [18] San Marchi C, Somerday BP, Zelinski J, Tang X, Schiroki GH. Mechanical properties of duplex stainless steel 2507 after gas phase thermal precharging with hydrogen. *Metallurgical Mater Transaction A* 2007;38A:2763–75.
- [19] Bahrami A, Bourgeon A, Cheaitani M. Effect of strain rate and microstructure on fracture toughness of duplex stainless steel under hydrogen charging conditions. In: Proceedings of the ASME 2011 30th International Conference on Ocean, Offshore and Arctic engineering, Rotterdam, The Netherlands; 2011. p. 1–11.
- [20] Wang John Jy-An, Ren Fei, Tan Tin, Liu Ken. The development of in situ fracture toughness evaluation techniques in hydrogen environment. *Int J hydrogen energy* 2015;40:2013–24.
- [21] Wang Yanfei, Gong Jianming, Jiang Wenchun. A quantitative description on fracture toughness of steels in hydrogen gas. *Int J hydrogen energy* 2013;38:12503–8.
- [22] ASTM E1245-03. Standard practice for determining the inclusion or second-phase constituent content of metals by automatic image analysis. 2008.
- [23] ASTM E562-05. Standard test method for determining volume fraction by systematic manual point count. 2005.
- [24] DNV RP F112–08. Design of duplex stainless steel subsea equipment exposed to cathodic protection. 2008.
- [25] Ernst HA, Echaniz G, Bravo R, Perez T, Morales C, López Turconi G. Effect of different test variables on the KISSC value. *Corrosion* 2004. paper no 04132.
- [26] Cravero S, Bravo R, Ernst H, Cancio MJ, Perez T. Evaluation of testing condition effects on the resistance to sulfide stress cracking. *Nace Conf Expo* 2009. Paper no 09309.